Alkoxy-Substituted Poly(p-phenylene 1,3,4-oxadiazole)s: Synthesis, Chemical Characterization, and Electro-Optical Properties

ARTICLE *in* CHEMISTRY OF MATERIALS · MARCH 2002

Impact Factor: 8.35 · DOI: 10.1021/cm011134u

Alkoxy-Substituted Poly(*p*-phenylene 1,3,4-oxadiazole)s: Synthesis, Chemical Characterization, and Electro-Optical Properties

M. Gillo,[†] P. Iannelli,[‡] P. Laurienzo,*[,†] M. Malinconico,[†] A. Roviello,[§] P. Mormile,[∥] and L. Petti[∥,⊥]

Istituto di Chimica e Tecnologia dei Polimeri (ICTP)-CNR, Via Campi Flegrei, 34-80078 Pozzuoli, Naples, Italy, Dipartimento di Ingegneria Chimica e Alimentare, Università degli Studi di Salerno, via Ponte Don Melillo, I-84084 Fisciano, Italy, Dipartimento di Chimica, Università di Napoli "Federico II", via Cinthia 6, 80126 Naples, Italy, Istituto di Cibernetica-CNR, via Toiano 6, 80072 Arco Felice, Naples, Italy, and Physics Department, Trinity College, Dublin, Ireland

Received May 23, 2001. Revised Manuscript Received December 13, 2001

The synthesis of a series of conjugated aromatic polyoxadiazoles (POD*n*) characterized by having moderate chain flexibility and highly flexible lateral substituents is reported. The majority of these polymers are soluble in a mixture of chloroform and trifluoroacetic acid and have inherent viscosities up to 0.9 dL/g. The glass transition temperature, T_g, lies in the range 165−230 °C and depends on the side-chain length. The POD*n* show a good thermal stability in nitrogen up to 270 °C. Wide-angle X-ray diffractograms reveal a "comblike" organization of the polymeric chains. Homogeneous thin films of such a material were prepared by the spin-coating technique. Films spun on fused silica were characterized by spectroscopic analysis in the whole UV−vis−NIR range showing a high transmission in the NIR region which is the typical telecommunication band (1300−1500 nm). Furthermore, the refractive index and the film thickness have been measured using the coupled modes technique in a planar guiding structure having POD as the core. It has then been prepared a device consisting of the said polymer sandwiched between two electrodes on top of a glass substrate. The electron conductivity of the polymer has been found to be higher than that of terephthalic poly(1,3,4−oxadiazole).

Introduction

The discovery, at the end of the 1970s, that certain polymeric and organic materials, if opportunely treated, can conduct electricity almost as efficiently as copper,[1] sparked a general interest in electronic and optoelectronic devices made entirely from plastics or from simple organic materials. Among these, organic crystals composed of three (anthracene) to five (pentacene) linked rings of carbon atoms and fullerene systems (C_{60}) have been studied for their properties of superconductivity[2] For what concerns the polymers, electrically active polymers can be divided into two main groups: filled polymers and molecularly (inherently) conductive polymers. The first group can be viewed as pseudo-active as far as polymers are concerned, since the electrical properties come from the addition of particles of electrically conductive materials, usually carbon, aluminum, or steel. In this case, the polymer matrix functions simply as a forming and protective medium in which the particles provide the electrical properties.[3] The molecularly conductive polymers, instead, have the characteristic of contain alternate double or triple bonds or aromatic units in the main chain which can delocalize π electrons. In contrast, full saturated polymers have been classified as insulators and employed for their good properties as insulating materials.

The conductive polymers show values of the inherent electrical conductivity σ comprised between 10^{-5} and 10^{-15} Ω^{-1} cm^{-1}; in the range of σ between about 10^{-5} and 10^{-12} Ω^{-1} cm^{-1} they are classified as semiconductors[4] (the valence band is completely full and the conduction band is completely empty at the absolute zero of temperature, but they have an energy gap between the valence and conduction bands of no more than about 2 eV). Higher values, up to 10^3 Ω^{-1} cm^{-1} (which is typical of a metallic conductor), can be measured when the polymers are "doped" with charge transferring elements or compounds (extrinsic conductivity). These consist of either electron donors (alkaline metals) or electron acceptors (halogens, AsF_5).

* Correspondence author.
[†] Istituto di Chimica e Tecnologia dei Polimeri (ICTP)-CNR.
[‡] Università degli Studi di Salerno.
[§] Università di Napoli "Federico II".
[∥] Istituto di Cibernetica-CNR.
[⊥] Trinity College.

(1) Chiang, C. K.; Fincher, C. R.; Park, Y. W.; Heeger, A. G.; Schirakawa, H.; Louis, E. J.; Gau, S. C.; MacDiarmid, A. G. *Phys. Rev. Lett.* **1977**, *39*, 1098.
(2) Phillips, P. *Nature* **2000**, *406*, 687.
(3) *Science and Applications of Conducting Polymers*; Salaneck, W. R., Clark, D. T., Samuelson, E. J., Eds.; Adam Hilger: Bristol, U.K., 1991.
(4) Hide, F.; Dìaz-Garcìa, M. A.; Schwartz, B. J.; Andersson, M. R.; Pei, Q.; Heeger, A. H. *Science* **1996**, *273*, 1833.

10.1021/cm011134u CCC: $22.00
Published on Web 03/28/2002

Polyacetylene is the most widely investigated electroactive polymer, but a large number of other conjugated polymers of high interest are now also established.[5−13] Of these, great efforts are devoted to polypyrrole, poly(*p*-phenylene), polythiophene, poly(*p*-phenylene vinylene), and, more recently, polyaniline. Poly(*p*-phenylene sulfide) is an example of a nonconjugated chain that produces conductivity when doped, in the semiconductor range. A large number of potential applications have been foreseen for these polymers, as, for instance, regulating photovoltaics of transduction of the solar energy in electric energy or less sophisticated applications as low cost diodes, thermistors, chemical sensors, etc.

One of the main goal of the research on conductive polymers is to increase the long-term stability and the ability to reproduce them. For what concerns the polyacetylene, the major limit is represented by its instability to the degrading action of the oxygen. The material exposed to the air is quickly oxidized, loosing the characteristics of crystallinity, metallic brightness, and flexibility (it becomes brittle) and, if doped, of electrical conductivity. Concerning the aromatic polymers, the major limit is represented by the insolubility and infusibility that make them hardly processable.

Poly(*p*-phenylene-1,3,4-oxadiazole) (POD), in comparison to polyacetylene, introduces an excellent thermal and oxidative resistance (thermal degradation: 450 °C < T < 500 °C).[14,15] Furthermore, the highly conjugated chain with a π electrons population characterized by high mobility makes POD appealing for application in the electrooptical field. Also, for the POD, the consideration holds on its intractability: it is infusible and it is soluble only in strong mineral acids such as sulfuric and poly(phosphoric acids).

Recently, numerous studies have been focused on the possibility to improve the solubility and the processability of polymers introducing flexible side ramifications like alkylic[16,17] or alkoxylic[18−25] chains. It is interesting to notice that the peculiar structure of the main chain of such polymers is not altered by the insertion of ramifications. In general, however, not only are such "interferences" limited to improve solubility and lower the melting and glass transition temperatures, but also they influence other properties such as the mechanical properties and the thermal stability.

In the present work, we prepared aromatic alkoxy-substituted polyoxadiazoles (POD*n*) having the general formula:

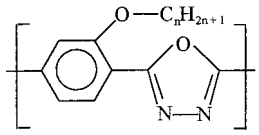

with n = 2, 5, 8, 10.

The introduction of large and flexible side chains is expected to improve the solubility of POD in organic solvents. Another important aspect is the constitutional disorder of the polymers introduced by the side chains that can lower the crystallinity of POD and induce the formation of mesophases, an important property for electrooptical applications of the material.

The polymers have been characterized by elemental analysis, FTIR and ^{1}H NMR spectroscopy, and thermal (DSC and TGA), dynamic-mechanical (DMTA) and wide-angle X-ray analyses.

Electrical and optical characterizations have been performed on thin and homogeneous films of POD*n* prepared by spin-coating technique.

Experimental Section

Materials. Na_2CO_3, K_2CO_3, LiCl (Aldrich) were dried under vacuum at 100 °C for 24 h just before use.

Reagents used without further purification: (i) 2-aminoterephthalic acid and KOH, from Fluka; (ii) 1-bromoethane, 1-bromopentane, 1-bromooctane, 1-bromodecane, $NaNO_2$, $SOCl_2$, and $POCl_3$, from Aldrich; (iii) hydrazine hydrate, from Sigma.

N,*N*′-Dimethylacetamide (Aldrich) was anhydrified and stored over 4 Å molecular sieves. All the other solvents were used as received.

Synthesis of Precursors. Hydroxyterephthalic acid, 2-alkoxyterephthalic acids and 2-alkoxyterephthaloyl dichlorides (**1**) have been synthesized according to previously reported procedures.[18]

Synthesis of 2-Alkoxyterephthaloyldihydrazides (DHD). DHD were prepared by reaction of 2 mL of corresponding dichloride (**1**) with a large excess (40 mL) of methanol at reflux for 1 h. After this time, the unreacted methanol was removed by Rotovap; then, 25 mL of absolute ethanol and 25 mL of hydrazine hydrate were added. The reaction was carried out at reflux for 1 h. The product precipitates after cooling; it was filtered, washed with water, dried at 90 °C in a vacuum and stored on P_2O_5 (yield > 90%). Four dihydrazides with different values of n in the alkoxylic chain have been prepared and coded DHD*n*, with n = 2, 5, 8, 10.

(5) Mort, J., Pfister, G., Eds. *Electronic Properties of Polymers*; J. Wiley & Sons: New York, 1982.
(6) Kryzewski, M. Ed.; *Semiconducting Polymers*; PWN-Polish Scientific Publishers: Warszawa, 1980.
(7) Gau, S. C.; Milliken, J.; Pron, A.; McDiarmid, A. G.; Heeger, A. J. *J. Chem. Soc., Chem. Commun.* **1979**, 662.
(8) McDiarmid, A. G.; Heeger, A. J. *Synth. Met.* **1980**, *1*, 101.
(9) Shacklette, L. W.; Chance, R. R.; Ivory, D. M.; Miller, G. G.; Baughman, R. H. *Synth. Met.* **1979**, *1*, 307.
(10) *Handbook of Conducting Polymers*; Skotheim, T. A., Ed.; Dekker: New York.
(11) Shacklette, L. W.; Elsenbaumer, R. L.; Chance, R. R.; Eckhardt, H.; Frommer, J. E.; Baughman, R. H. *J. Chem. Phys.* **1981**, *75*, 1919.
(12) Kobayashi, M.; Chen, J.; Chung, T. C.; Moraes, F.; Heeger, A. J.; Wudl, F. *Synth. Met.* **1984**, *9*, 77.
(13) Yamamoto, T.; Sanechika, K.; Yamamoto, A. *J. Polym. Sci., Polym. Lett. Ed.* **1980**, *18*, 9.
(14) Tsuitsui, T.; Fukuta, Y.; Hara, T.; Saito, S. *Polym. J.* **1987**, *19*, 719.
(15) Calandrelli, L.; Immirzi, B.; Kummerlowe, C.; Malinconico, M.; Riva, F. *Recent Res. Dev. Polym. Sci.* **1998**; *2*, 569.
(16) Stern, R.; Ballauff, M.; Lieser, G.; Wegner, G. *Polymer* **1991**, *11*, 2096.
(17) Huang, W.; Yu, W. L.; Meng, H.; Pei, J.; Li, S. F. Y. *Chem. Mater.* **1998**, *10*, 3340.
(18) Caruso, U.; Pragliola, S.; Roviello, A.; Sirigu, A.; Iannelli, P.; *Macromolecules* **1995**, *28*, 6089.
(19) Centore, R.; Roviello, A.; Sirigu, A. *Macromol. Chem. Phys.* **1994**, *195*, 3009.
(20) Kricheldorf, H. R.; Engelhardt, J. *Makromol. Chem.* **1990**, *191*, 2017.
(21) Ballauff, M.; Schmidt, G. M. *Makromol. Chem., Rapid Commun.* **1987**, *8*, 93.
(22) Lee, K. S.; Kim, H. M.; Rhee, J. M.; Lee, S. M. *Makromol. Chem.* **1991**, *192*, 1033.
(23) Bao, Z.; Chen, Y.; Cai, R.; Yu, L. *Macromolecules* **1993**, *26*, 5281.
(24) Rodriguez-Parada, J. M.; Duran, R.; Wegner, G. *Macromolecules* **1989**, *22*, 2507.
(25) Harkness, B. R.; Watanabe, J. *Macromolecules* **1991**, *24*, 6759.

Melting temperatures (°C): 202 (DHD2), 148 (DHD5), 137 (DHD8), 143 (DHD10). ^{1}H NMR (DMSO-d_6) of DHD5 (as an example): δ 9.88 (s, 1H), 9.16 (s, 1H), 7.68 (d, 1H), 7.48 (d, 2H), 4.54 (s, 2H), 4.11 (m, 2H), 1.76 (m, 2H), 1.37 (m, 4H), 0.89 (t, 3H).

Polymer Synthesis. (a) 2-Octanoxyterephthalicpolyhydrazide (PHZ8). A 1.50 g (4.66 mmol) sample of octanoxyterephthaloyldihydrazide was dissolved in 48.00 g of a DMAc solution containing LiCl (5 wt %), in a glass reactor equipped with mechanical stirring. The solution was cooled at 0 °C, and then a stoichiometric amount of the corresponding dichloride was added. The reaction was carried out for 3 h at 0 °C and for 12 h at room temperature. At the end of the reaction, the solution is highly viscous. The white polymer is recovered by precipitation with 200 mL of methanol, separated, washed several times with water and dried for 12 h under vacuum at 110 °C (yield $\sim$ 90%).

(b) 2-Octanoxyterephthalicpolyoxadiazole (POD8). A 1.00 g sample of PHZ8 was refluxed in 25 mL of $POCl_3$ for 6 h, and then the reaction mixture was slowly poured into 200 mL of water. The reaction mixtures are always turbid or cloudy. The precipitated yellow polymer was isolated by filtration and successively washed with water, ethanol, and ether and finally dried under vacuum at room temperature (yield $\sim$ 100%).

Techniques. The inherent viscosities of polymers were determined with an Ubbelhode viscometer at 25 °C and c = 0.3 g dL^{-1} in dimethyl sulfoxide (DMSO) for polyhydrazides and in a mixture of chloroform and trifluoroacetic acid (TFA) for polyoxadiazoles.

The infrared spectra were recorded using a Perkin-Elmer System 2000 FTIR spectrophotometer on films obtained by solution casting.

The ^{1}H nuclear magnetic resonance (NMR) spectra were obtained using a Bruker-300 MHz spectrometer operating on polyhydrazide solution in dimethyl sulfoxide-d_6 (DMSO-d_6) and polyoxadiazole solution in a mixture of $CDCl_3$/CF_3COOD.

Calorimetric analysis was performed on 10−15 mg of sample using a Mettler DSC-30 differential scanning calorimeter (DSC) from 30 to 250 °C and with a heating rate of 20 °C/min. The glass transition temperature, T_g, was taken at the midpoint of the transition step in the second heating run after quenching.

Thermogravimetric analysis (TGA) was carried out on a Mettler TC-11 thermobalance under nitrogen at a heating rate of 20 °C/min from 40 to 600 °C.

Dynamic mechanic thermal analysis (DMTA) was carried out on films, obtained by solution casting, using a Polymer Laboratories MK III instrument. The frequency used was 10 Hz from −100 to +300 °C and the heating rate was 3 °C/min in tensile mode.

Optical microscopy analysis has been performed on thin films with an optical microscope Zeiss Mc 100 equipped with a Linkman Tms 901 apparatus for the control of temperature and an hot stage Linkman Thms 600.

Wide-angle X-ray (WAXS) powder patterns were recorded on a Philips PW 1711 diffractometer using Ni-filtered Cu Kα radiation.

Devices for electron conductivity measurements were prepared on l2 mm square glass substrates. The bottom aluminum contact was sputtered to a thickness of 75 nm using an RF sputtering system. Four films of POD8 were spun. The films were desiccated in a vacuum at 70 °C for 2 h to remove any remaining solvent. The top aluminum contacts were deposited using a thermal evaporator. The mask used for depositing the top contacts allowed for six devices per substrate. Current−voltage measurements were taken under vacuum using a Keithley 2400 sourcemeter, interfaced using *Quick Basic* software with a computer.

Spectral analysis in the UV−vis−NIR range was performed on solvent-cast films using a JASCO V-570 spectrophotometer. Thin and homogeneous films were prepared from solutions onto different supports using a SUSS RC5 spin-coater. Measurements of refractive index were performed using an He−Ne laser beam (λ = 632.8 nm), TE polarized. The refractive index of the substrate (silica fused) is 1.457 and the prism index is 1.756 at the same wavelength. The prism angle between the incident face and the prism is 62.8°. We made measurements on POD8 films with different thickness ranging from 0.7 to 1.5 μm.

Results and Discussion

Polymer Synthesis and Characterization. Aromatic polyoxadiazoles can be prepared by the "one-step" method, starting from aromatic diacids (or the corresponding nitrile, amide, or ester) and hydrazine sulfate in oleum or poly(phosphoric acid).[26−28] Alternatively, they can be synthesized by cyclodehydration of polyhydrazide precursor; such reaction can be thermally (T > 300 °C) or chemically (using dehydrating agents like poly(phosphoric acid) or $POCl_3$) activated ("two-step" method).[29,30]

In the present work, as the alkoxylic ramifications are sensitive to acid hydrolysis and, furthermore, they are not very stable at temperature close to 300 °C, POD*n* were prepared by the "two-step" method using $POCl_3$ as a dehydrating solvent, according to the route depicted in Scheme 1.

The solubility tests for PHZ*n* and POD*n* are reported in Table 1. As can be seen from the table, in the case of POD*n* it is necessary to add a certain amount of a strong organic acid, like trifluoroacetic or methanesulfonic acid, to dissolve them partially or totally in chlorinated solvents. The volume ratio of the TFA/$CHCl_3$ mixture has to be at least 1/2 to dissolve POD2, 1/3 for POD5, 1/4 for POD8, and 1/7 for POD10. The maximum concentration of this last polymer in the said mixture is 150 g/L.

Inherent viscosities of PHZ*n* were obtained in DMSO. Although it is not possible to compare the values with literature data, it is possible to say that the obtained values (0.9−1.4) are typical, for condensation polymers, of medium to high molecular weights. The η_{inh} of corresponding POD*n*, obtained in the proper $CHCl_3$/TFA ratio, are always reduced in comparison with the parent PHZ. This can be attributed partly to the different solvent and partly to the different chemical structure of POD. The side-chain length does not have a relevant influence on the inherent viscosity of both POD*n* and PHZ*n*.

The chemical structures of the PHZ*n* and POD*n* can be confirmed by FTIR, elemental analysis, and ^{1}H NMR spectroscopy.

In Figure 1, a comparison between the FTIR spectra of POD5 and PHZ5 is shown as an example. After the treatment with $POCl_3$, the intensive absorption peaks at around 1620 and 1510 cm^{-1} arising from carbonyl groups of polyhydrazide and those at 3200−3300 cm^{-1} due to the N−H stretching almost disappear. Meanwhile, the characteristic bands of the oxadiazole ring at 1558 cm^{-1} (C═N stretching) and at 1076 and 1229 cm^{-1} (═C−O−C═ stretching) appear. Other character-

(26) Morton, A. A.; Leitsinger, R. L. *J. Am. Chem. Soc.* **1945**, *67*, 1537.
(27) Iwakura, Y.; Uno, K.; Hara, S. *J. Polym. Sci.* **1965**, *A 3*, 45.
(28) Neugebauer, W. Japanese Patent, 256,946, 1959.
(29) Frazer, A. H.; Wallenberger, F. T. *J. Polym. Sci.* **1964**, *A 2*, 1157.
(30) Schulze, B.; Bruma, M.; Brehmer, L. *Adv. Mater.* **1997**, *9*, 601.

Scheme 1. Synthetic Route[a]

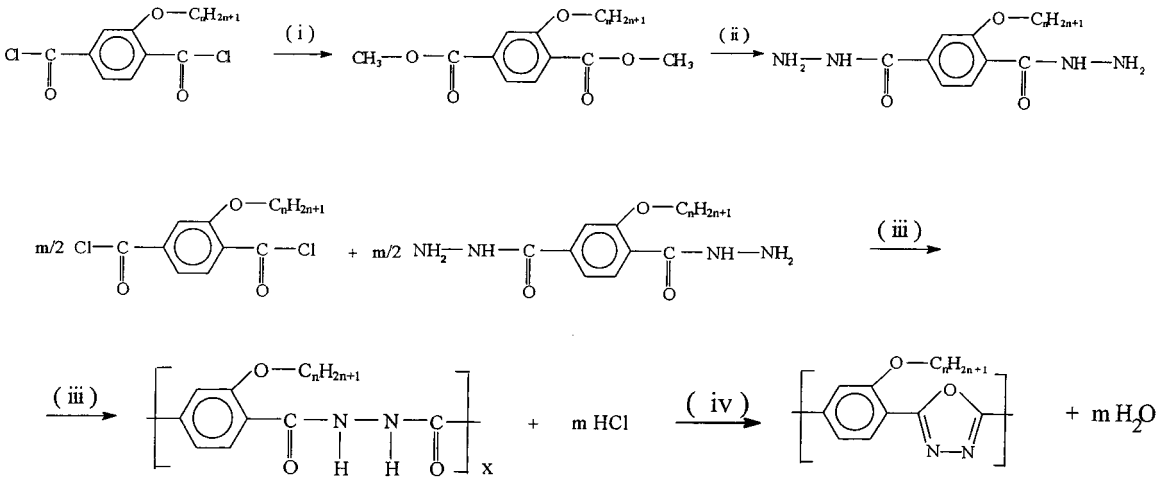

[a] Key: (i) MeOH, 1 h, 70 °C; (ii) EtOH + $NH_2NH_2 \cdot H_2O$, 1 h, 80 °C; (iii) DMAc, 5% LiCl, 0−4 °C; (iv) $POCl_3$, 6 h, 125 °C.

Table 1. Inherent Viscosity (η_{inh}) and Solubility of PHZ*n* and POD*n*

		solubility[a]					
polymer code[b]	η_{inh}[c] (dL/g)	DMSO	$CHCl_3$	TFA	$CHCl_3$/ TFA	trichloro-ethane/ TFA	$CHCl_3$/ CH_3SO_3H
PHZ2	0.91	++	−	++	++	++	++
PHZ5	1.37	++	−	++	++	++	++
PHZ8	1.31	++	−	++	++	++	++
PHZ10	1.35	++	−	++	++	++	++
POD2	0.71	−	−	−	++	−	−
POD5	0.89	−	−	−	++	+−	+−
POD8	0.92	−	−	−	++	+−	+−
POD10	0.96	−	−	−	++	+−	+−

[a] Key: ++ = soluble; +- = partially soluble; − = insoluble. [b] 2, 5, 8, and 10 referred to the number of C atoms of the alkoxylic side chain. [c] Solvent: DMSO (PHZ*n*); $CHCl_3$/TFA; volume ratio, 2/1(POD2), 3/1 (POD5), 4/1 (POD8), and 7/1 (POD10).

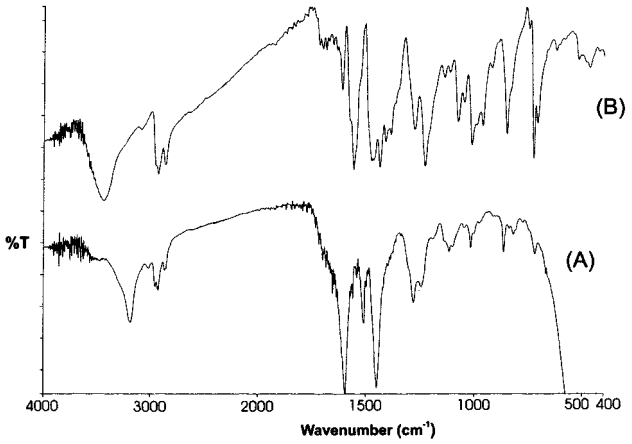

Figure 1. FTIR spectra of PHZ5 (A) and POD5 (B).

istic peaks include secondary absorptions at 726 and 850 cm^{-1}.[12] These results indicate that the cyclization reaction is not complete. This may be attributed to the scarce solubility of polyhydrazide precursors and of their corresponding polyoxadiazoles in $POCl_3$. No significative variations of spectral data have been evidenced in the other polymers.

The results of elemental analysis for PHZ*n* and POD*n* polymers are listed in Table 2, and they show good agreement with the expected values. The slightly higher

Table 2. Elemental Composition of the Polymers[a]

sample	C (%)	H (%)	N (%)	O (%)
PHZ2	58.29 (58.25)	5.20 (4.85)	12.90 (13.54)	23.61 (23.36)
POD2	63.61 (63.83)	4.36 (4.26)	14.74 (14.89)	17.29 (17.02)
PHZ5	62.98 (62.90)	6.43 (6.45)	11.14 (11.29)	19.45 (19.36)
POD5	67.03 (67.83)	6.68 (6.09)	11.91 (12.17)	14.38 (13.91)
PHZ8	65.61 (66.21)	8.01 (7.59)	9.23 (9.66)	17.15 (16.54)
POD8	69.98 (70.59)	7.47 (7.35)	9.85 (10.29)	12.70 (11.77)
PHZ10	67.62 (67.92)	8.30 (8.18)	8.74 (8.81)	15.34 (15.09)
POD10	71.00 (72.00)	8.15 (8.00)	9.11 (9.33)	11.74 (10.67)

[a] Figures in parentheses refer to theoretical values.

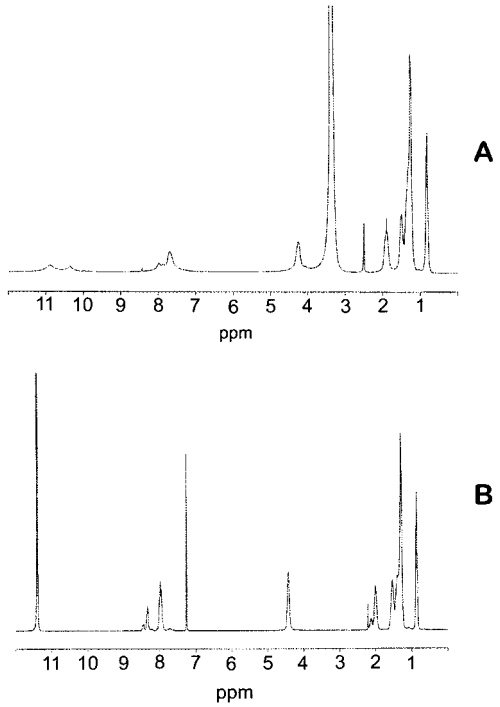

Figure 2. ^1H NMR spectrum of PHZ8 (A) and of POD8 (B).

contents of hydrogen and oxygen can be attributed to the absorbed water in PHZ8, as well as the incompleteness of the cyclodehydration in the case of POD8.

The ^1H NMR spectra of PHZ8 and POD8 are exhibited in Figure 2 (parts A and B) as example, and the relative chemical shifts are listed in Table 3. The chemical shifts and the relative intensities of the signals are in agree-

Table 3. ^{1}H NMR Chemical Shifts (ppm) of PHZ8 in d_6-DMSO and POD8 in $CDCl_3/CF_3COOD$

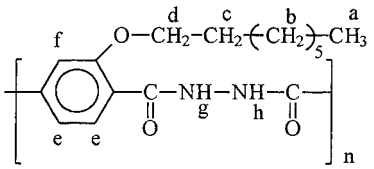

chemical group	δ (ppm) PHZ8	δ (ppm) POD8
CH_3 (a)	0.82 (t)	0.86 (t)
CH_2 (b)	1.40 (m)	1.42 (m)
CH_2 (c)	1.90 (m)	2.02 (m)
CH_2 (d)	4.27 (t)	4.42 (t)
aromatic (e)	7.68 (d)	8.02 (d)
aromatic (f)	7.92 (d)	8.35 (d)
NH (g)	10.37 (s)	
NH (h)	10.90 (s)	

Table 4. Glass Transition (T_g), α Transition (T_α) and Degradation (T_d) Temperatures of PHZ*n* and POD*n*

sample	T_g (°C) DSC	T_g (°C) DMTA	T_α (°C) (DMTA)	T_d (°C) (TGA)
PHZ2	240			300
PHZ5	234			300
PHZ8	202	205	−26	280
PHZ10	190	196	−25	250
POD2	231			340
POD5	205			340
POD8	173	*a*	−24	320
POD10	165	*a*	−24	300

[a] Not clearly detectable.

ment with the proposed structures for all the PHZ*n* and POD*n*.

Thermal and Thermogravimetric Analysis. DSC experiments in the first (i.e., on the material as prepared) and second (after cooling at 20 °C/min) heating runs show that the polymers do not have any melting transition. The thermograms revealed, instead, a glass transition for POD*n* and PHZ*n* strongly dependent on the side-chain length (see Table 4). In particular, the T_g values decrease with increasing the side-chain length, in agreement with an increased flexibility of the whole polymer. At temperatures above 300 °C, the PHZ*n* and POD*n* show an exothermic peak which, according to TGA analysis, is due to thermal decomposition.

TGA curves revealed that all the polymers are stable until at least 250 °C in nitrogen. Obviously, the thermal stability increases at decreasing chain length, going from 250 (PHZ10) to 300 °C (PHZ2). In Table 4, the degradation temperatures, taken as the temperatures at which the weight loss starts, are reported. The PHZ*n* show a fast weight loss around 300 °C (see Figure 3 as example) which is attributed to the loss of water due to the cyclodehydration reaction which happens during heating. Anyway, as this weight loss corresponds to more than 20%, it cannot be attributed only to evolved water (which should be around 10% for complete cyclization). A possible explanation is the simultaneous occurrence of degradation of alkoxy aliphatic chains. The overlapping of the two phenomena hinders the possibility to cyclize the PHZ*n* by heating.

Finally, POD*n* showed degradation temperatures higher than the corresponding PHZ*n* according to the better thermal stability of oxadiazole ring.

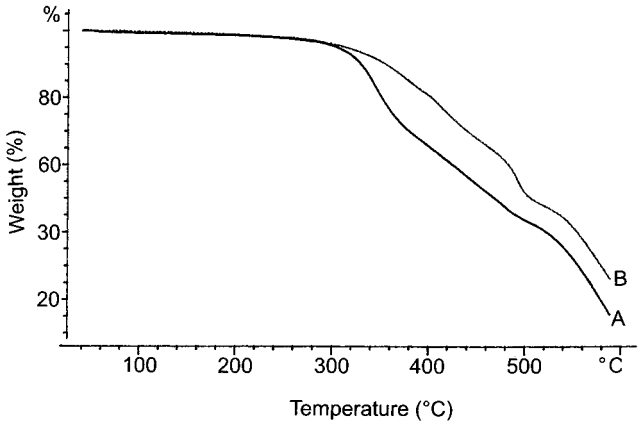

Figure 3. TGA curves for PHZ5 (A) and POD5 (B).

Dynamic-Mechanical Analysis. Dynamic-mechanical measurements were performed only on PHZ8, POD8, PHZ10, and POD10 films, and the plots of log E' and tan δ vs the temperature are reported in Figure 4. Unfortunately, the other samples were not analyzed with this technique because they were too brittle.

In the analyzed range of temperatures, two molecular relaxations are detectable. The first transition, reported as T_α in Table 4, at about −25 °C, can be ascribed to the molecular relaxation of the high flexible aliphatic side chains. The second transition, in the range of 190−220 °C, well visible in the PHZ*n* samples, can be associated with the glass transition.

Some differences are evident in the PHZ*n* and POD*n* samples. First, in PHZ*n* samples the peak of the loss factor tan δ in the region of the glass transition is well-defined and the modulus values are always higher than the correspondent POD*n* samples. This can be explained in terms of a strong interaction between N−H bonds and C═O bonds present in PHZ*n* samples and not present in POD*n* samples as effect of the cyclization. This interaction can account for the higher modulus level in the region of the glass transition for PHZ*n* samples. In the POD*n* samples, tan δ increases at lower temperatures, and also this can be related to the reduced interchain interaction. Finally, the broadness of tan δ at temperatures higher than 70 °C can be due to the fact that the cyclization is not complete, and therefore, the POD*n* samples still contain a certain amount of PHZ*n*.

X-ray Diffraction Analysis. X-ray diffraction data for PHZ*n* and POD*n* (referred to polymers as obtained from polymerization and from reaction with $POCl_3$, respectively) are reported in Table 5.

Powder diffractograms for POD*n* show only two sharp and one broad diffraction peaks (diffractogram of POD5 is showed in Figure 5). Annealing at a temperature higher than the glassy temperature does not induce crystallization and the diffraction spectra remain the same.

According to the following discussion, the diffraction data are accountable for a "molecular layers" arrangement, where the side chains shows a planar extended conformation (see Figure 6). Oriented samples, when available, provide more information than unoriented ones. In fact, in the experimental pattern of an oriented sample, diffraction spots can be unambiguously classi-

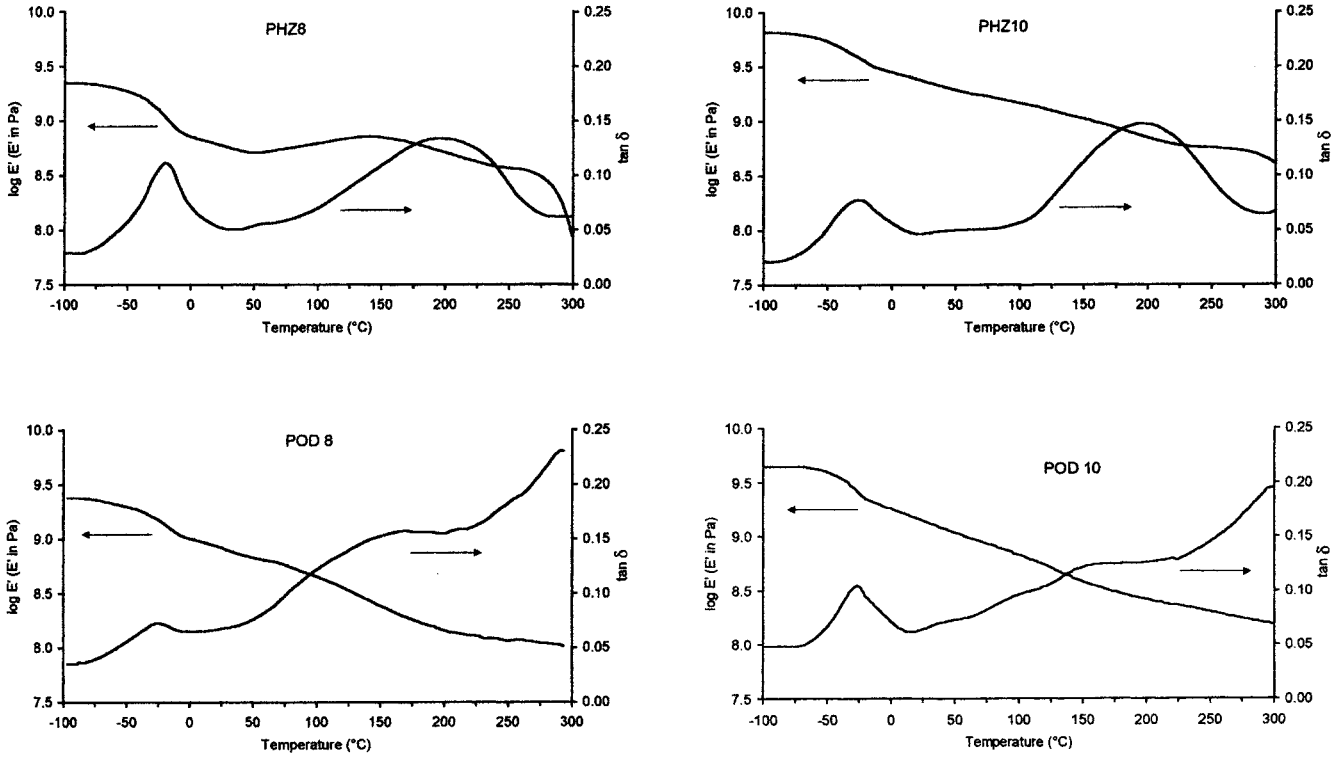

Figure 4. DMTA curves for PHZ8, POD8, PHZ10 and POD10.

Table 5. X-ray Data for PHZ*n* and POD*n*

polymer	2θ (deg)	d_{hkl} (Å)
PHZ2	9.25 ± 0.05	9.6 ± 0.2
	25.85 ± 0.05	3.4 ± 0.1
PHZ5	6.15 ± 0.05	14.4 ± 0.2
	23.10 ± 0.05	3.8 ± 0.1
PHZ8	4.00 ± 0.05	21.1 ± 0.2
	21.25 ± 0.05	4.2 ± 0.1
PHZ10	3.70 ± 0.05	24.0 ± 0.2
	20.9 ± 0.05	4.2 ± 0.1
POD2	9.40 ± 0.05	9.4 ± 0.2
	25.55 ± 0.05	3.5 ± 0.1
POD5	6.60 ± 0.05	13.4 ± 0.2
	22.15 ± 0.05	4.0 ± 0.1
	26.45 ± 0.05	3.4 ± 0.1
POD8	5.25 ± 0.05	16.9 ± 0.2
	20.60 ± 0.05	4.3 ± 0.1
	26.45 ± 0.05	3.4 ± 0.1
POD10	4.65 ± 0.05	19.0 ± 0.2
	20.30 ± 0.05	4.4 ± 0.1
	26.35 ± 0.05	3.4 ± 0.1

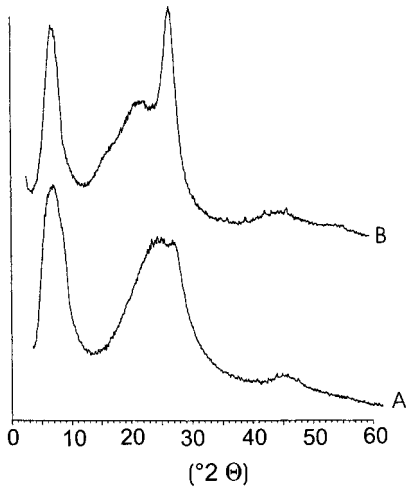

Figure 5. X-ray powder pattern of PHZ5 (A) and POD5 (B).

fied as equatorial or meridional reflections. In this case, the molecular packing model can be easily verified. Unfortunately, oriented samples cannot be drawn because of high T_g and relatively low degradation temperatures: the viscosity is very high (the materials do not soften above T_g) and we should go well above T_g to impart orientation. The hypothesized layer structure well explain the difficulty of the chains to flow; in fact, the films break without achieving orientation. Attempts of preparing oriented samples by spinning from solution also failed. It is worth to mentioning that optical measurements in polarized light on POD*n* films show evidence of a diffuse birefringence which disappears around 280−300 °C. The birefringence is reversible, but the transition is accompanied by decomposition.

The diffraction peak at 26° is equal for all the samples and corresponds to a *d* spacing of 3.4−3.5 Å: for the layered packing model, this is the spacing between adjacent chains (layer thickness), and furthermore, it coincides with the typical distance observed between aromatic planes in aromatic systems (e.g., graphite). The intense diffraction peak at low angle shifts to lower values increasing the side-chain length. The corresponding *d* spacing, that increases linearly with the side-chain length (Figure 7), corresponds to the width of the macromolecular layer. This arrangement allows the segregation between the flexible side chains and the rigid main chains that are incompatible each other. On average, there is a spacing increment of 9.6 Å going from POD2 to POD10, which corresponds to an increment of 1.20 Å for methylene. To justify this result the aliphatic segment of the side group should adopt almost the *zigzag* planar conformation in the plane of the molecular layer. The diffuse halo with a spacing of 4.0−4.4 Å observed for POD5, POD8, and POD10 can be attributed to the interactions of alkoxylic side chains that occupy

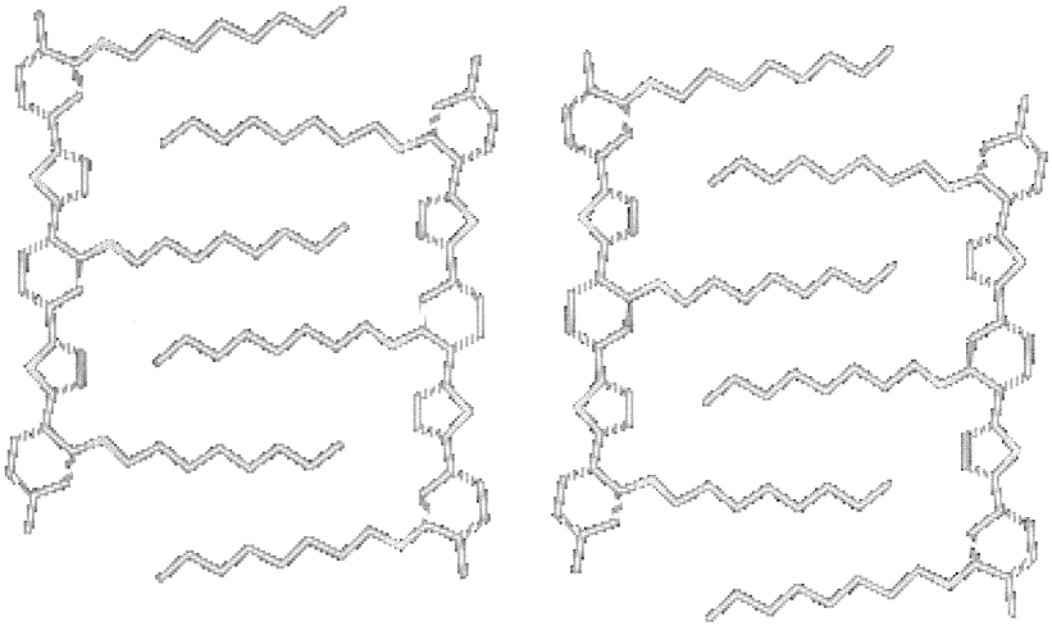

Figure 6. Molecular layer packing.

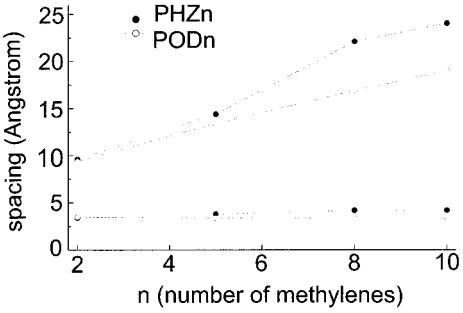

Figure 7. *d* spacing vs the number of methylenes (*n*) of alkoxy side chain for PHZ*n* and POD*n*.

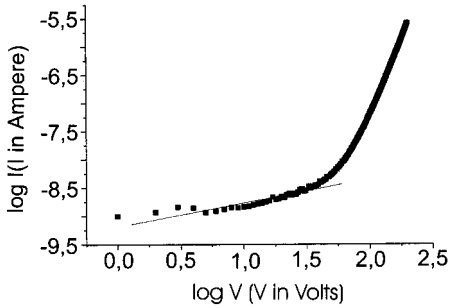

Figure 8. The log *I* vs log *V* curve of POD8.

the space into the layer. According to the diffuse character of the halo and the absence of further diffraction peaks, the flexible side groups, even if with the most extended conformation, are not packed in an ordered fashion. The very broad peak at about 43°, which is detectable in both PHZ*n* and POD*n*, is probably attributable to the side group.

For PHZ*n* we cannot draw a clear packing hypothesis. PHZ2 shows an intense diffraction peak at 26°, while PHZ8 and PHZ10 show a diffuse halo. PHZ5 presents an intermediate situation (Figure 5). The intense peak at low angle shifts to lower values (increasing the side-chain length) in a different way with respect POD*n* (Figure 7). In fact, in the case of PHZ*n*, going from PHZ2 to PHZ10, there is a spacing variation of 14.4 Å, corresponding to an increment of 1.80 Å for methylenic unit: this is not in agreement with the layered structure of POD*n*. Furthermore, the spacing increment is not linear.

Electron Conductivity. To measure the electron conductivity of a material, a voltage is applied to a thick film and the variation of the intensity current is recorded.

In Figure 8, we present the best curve log *I* (intensity) as a function of log *V* (voltage) for one of our devices prepared with a POD8 sample. Such a curve shows a linear trend up to the critical voltage V_c. From that value, a quadratic behavior of the current intensity is observed. In the linear regime, according to the theory, the following condition is verified:

$$\log I = \log V + \log G \qquad (1)$$

where *G* is the material conductance. The conductivity is related to the conductance by

$$\sigma = Gd/A \qquad (2)$$

with *A* is the active area and *d* the thickness of the polymeric film, determined by a profilometer.

Table 6. Experimental Results and Values of Conductance (*G*) and Electron Conductivity (σ)

device	A (m^2)	d (μm)	G (S)	σ (S/cm)
1	4.00×10^{-6}	1.6	4.40×10^{-10}	1.76×10^{-12}
2			5.37×10^{-10}	2.15×10^{-12}
3			5.37×10^{-10}	2.15×10^{-12}
4			4.79×10^{-10}	1.91×10^{-12}
5			3.71×10^{-10}	1.50×10^{-12}
6			3.63×10^{-10}	1.45×10^{-12}

In Table 6, we report the experimental data for all the devices prepared. The average value of the electron conductivity obtained is $\sigma = (1.8 \pm 0.2)\ 10^{-12}$ S/cm, which is higher than that of POD ($\approx 10^{-16}$ S/cm). This result is in agreement with what reported by other authors on nonconjugated polymers containing 1,3,4-

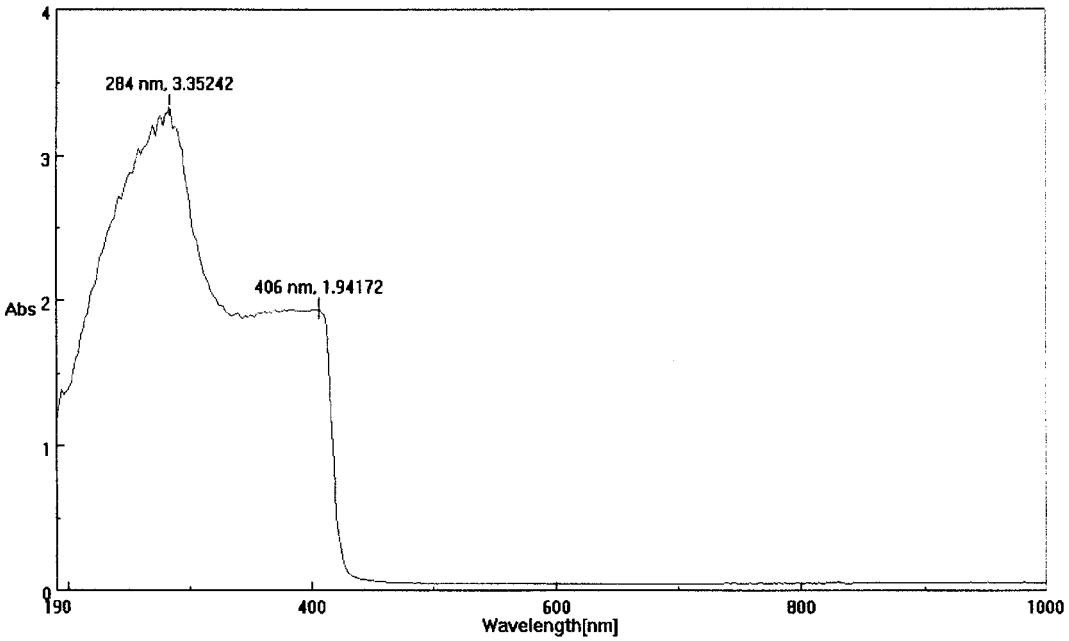

Figure 9. Total absorbance spectrum of POD8 in the range 200−1000 nm.

oxadiazole and/or -tiadiazole rings.[31−33] In our case, a further explanation for the good electron conductivity, despite the fact that POD8 is not totally cyclized, is the occurrence of a keto−enolic tautomerism of the residue hydrazidic groups. The enolic form is favored by the possibility of conjugation with the aromatic rings, so increasing the effective conjugated length of the main chain.The electron conductivity should be enhanced of orders of magnitude by adding a proper dopant. Preliminary doping tests on POD8 using iodine (I_2) like dopant agent have shown that, after exposure to iodine vapors, at room temperature and atmospheric pressure, films of POD8 adsorb a very high amount of I_2 (35 wt %). The process is reversible: after a few days, the films return to their original weight with an excess of 2% only, suggesting that the I_2 is not covalently bonded.

Optical Properties. *(a) Spectral Analysis.* To evaluate the optical properties of POD*n*, a spectral analysis in the UV−vis−IR region from 200 to 2500 nm has been performed. The employed spectrophotometer allows one to obtain the transmission, reflection, and absorption spectrum of the material with light both collimated and scattered. In Figure 9, the absorbance spectrum of a POD8 film in total light in the range 200−1000 nm is shown. The main feature of this curve is the very high absorbance in the range 200−406 nm with a sharp slope and a high constant transmission from 406 nm up to 2500 nm. The very strong absorption in the UV region is due to an electronic transition $\pi \rightarrow \pi^*$. In fact, such a polymer presents a huge π-electron population in the main chain. This behavior suggests the possibility of employing such a material as an UV optical filter or as a coating for shielding elements to be employed in the industrial and medical field.

Another relevant feature is the high transmittivity in the NIR region which is, as well-known, the typical telecommunication band (1300−1500 nm). This last property makes POD*n* very attractive for preparing planar waveguides useful in integrated optics.

A quantitative measurement of the absorption has been done by evaluating the molar extinction coefficient ϵ of a polymer solution at $\lambda = 368$ nm, where the solution showed the maximum absorbance: a value of $\epsilon_{368} =$ (16900 ± 100) mol cm L^{-1} was obtained.

(b) Measurements of the Refractive Index. Toward device application, the refractive index is an important optical parameter of the material. Such a value allows to define also the potential applications in different fields of interest. To measure the refractive index of POD*n*, a traditional technique *(m-line technique)* has been employed, based on the light propagation in a planar waveguide coupled by a prism.[34] The prism coupler provides a fast, accurate and reliable method for determining the refractive index and thickness of thin dielectric films. POD8 films have been spin-coated onto fused silica substrates and characterized by the prism coupling method in order to determine the refractive index. If the conditions for coupling a light beam at a prism−film interface in the TIR regime are satisfied, a modal propagation occurs into the planar waveguide. The modes number propagating depends on the thickness of the core, and as is well-known, the selection of the single mode occurs by the variation of the incident angle of the light beam at the prism face. Such a method allows one to selectively excite a particular mode of the waveguide.

The coupling angle which excites each mode is obtained by measuring the angle of incidence on the prism entrance face for which the *m*th mode is excited. A computational routine for the PC was used for evaluating the linear refractive indices and thickness of the guiding layer.

The calculated value of the refractive index is 1.568 ± 0.002. Such a value makes POD8 a useful

(31) Schopov, I.; Sinigerski, V. *Macromol. Chem.* **1992**, *193*, 1839.
(32) Sinigerski, V.; Kossmehl, G.; Mladenova, L.; Schopov, I. *Macromol. Chem. Phys.* **1996**, *197*, 1713.
(33) Sinigerski, V.; Madec, P. J.; Maréchal, E.; Schopov, I. *Macromol. Chem. Phys.* **1997**, *198*, 919.
(34) Tien, P. K.; Ulrich, B.; Martin, R. J. *Appl. Phys. Lett.* **1969**, *14*, 291.

polymeric material in order to prepare planar waveguide structures.

Conclusions

The introduction of alkoxy substituents onto the aromatic ring of otherwise highly rigid poly(*p*-phenylene 1,3,4-oxadiazole) is responsible for very significant changes in the chemical, as well as structural and optical, properties of the obtained polymers. The improved solubility in organic solvents of the modified polymers, one of the main target of this study, is achieved, although still the addition of a small amount of strong organic acid is necessary to stabilize the solutions. The structural organization in molecular sheets explains satisfactorily the WAXS data on POD*n*, while still some doubt remains about the interpretation of PHZ*n* WAXS data. Electrical conductivity, optical transmission, and refractive index of POD*n* demonstrate that this new family of polymers, although of not well-defined chemical structure due to the incompleteness of cyclodehydration, meets the requirements for application in many specialty fields, like semiconductors, planar waveguide, and telecommunication. It is evident, however, that more research will be necessary to fully exploit the potentialities of our modified polyoxadiazoles. Data on mechanical properties, dopability, and signal response time will be obtained and reported in future works.

Acknowledgment. The authors wish to express many thanks to Prof. W. J. Blau and to Mr. S. Lipson from Trinity College for the cooperation in electron conductivity analysis and to Mr. G. Romano from ICTP for technical support in DMTA analysis. The authors are also indebted to Dr. R. Russo from ICTP for the many helpful discussions on the interpretation of DMTA data.

CM011134U